Experimental investigation into the reduction of erosion of sand at high flow velocities

Foortse, Bjorn; Visser, Paul J.; Bisschop, Rik; Rhee, Cees Van

DOI
10.1680/jmaen.2019.6

Publication date
2019

Document Version
Accepted author manuscript

Published in
Proceedings of the Institution of Civil Engineers: Maritime Engineering

Reduction of erosion of sand at high flow velocities

Foortse, Visser, Bisschop and Van Rhee

Proceedings of the Institution of Civil Engineers
Pages 1–18

Keywords: Hydraulics & hydrodynamics/Granular materials/Slopes - erosion control

ice | **proceedings**

Experimental investigation into the reduction of erosion of sand at high flow velocities with a bentonite additive

Bjorn Foortse
MSc, Consultant Artificial Intelligence, Accenture Singapore, Singapore (Corresponding author: b.foortse@gmail.com)
Paul J. Visser
Dr, MSc, Associate Professor (retired), Faculty of Civil Engineering and Geosciences, Delft University of Technology, Delft, The Netherlands
Rik Bisschop
Dr, MSc, Senior Geotechnical Specialist, Ports & Hydraulic Structures, Arcadis Rotterdam, The Netherlands
Cees Van Rhee
Dr, MSc, Full Professor, Faculty of Mechanical Engineering, Marine Technology and Materials Science/Faculty of Civil Engineering and Geosciences, Delft University of Technology, Delft, The Netherlands

Significant reduction of the rate of erosion of a sand bed is obtained when sand is mixed with a small amount of bentonite. In previous experiments this behaviour has already been shown for relatively low flow velocities. In this case the erosion process is dominated by grain-by-grain erosion, which is characterized by low ratios of the erosion velocity and permeability ($v_e/k < 3$). It is unknown whether these reductions in the erosion process also occur at relatively high flow velocities, where dilatancy-reduced erosion dominates ($v_e/k > 3$). Experiments were executed in a tilting flume to investigate the erosion rate of sand-bentonite mixtures. In thirteen different tests, the dry volume percentage of the bentonite additive, the diameter of the sand particles and the depth-averaged flow velocity were varied. The depth-averaged flow velocities ranged from 1 to 2 m/s and all erosion tests were performed under supercritical flow conditions. The experiments show that the bentonite additive did not influence the strength characteristics of the sand, however, the permeability did decrease significantly. This proves that the significant decrease of the erosion rate was caused by the decrease of the permeability of the sand and that the test conditions were in the dilatancy-reduced regime.

Notation

A	tune parameter (-)
a	regression coefficient (-)
$B\%$	the percentage of added bentonite (%)
b	constricted width of the flume (m)
C_c	coefficient of curvature (-)
C_u	coefficient of uniformity (-)
c	empirical coefficient (-)
c_b	the near bed concentration (-)
c_f	dimensionless friction coefficient (-)
D	sediment diameter (mm)
D_*	dimensionless particle diameter (-)
D_{10}	particle diameter at which 10% of the weight of the grains is smaller (mm)
D_{30}	particle diameter at which 30% of the weight of the grains is smaller (mm)

D_{50}	median sediment diameter (mm)
D_{60}	particle diameter at which 60% of the weight of the grains is smaller (mm)
E	sediment pick-up flux (kg/m^2·s)
f	effectiveness ratio (-)
f_b	bed friction coefficient (-)
f_d	bulk friction coefficient (-)
f_w	wall friction coefficient (-)
g	gravitational acceleration (m/s^2)
h	flow depth (m)
$z_{b(n)}$	bed level at a specific time (m)
k	permeability (m/s)
k_l	permeability given a loose soil packing (m/s)
k_{sand}	permeability of the original sand (m/s)
n	Manning roughness coefficient (s/m$^{1/3}$)
n_b	bed-related Manning roughness coefficient (s/m$^{1/3}$)
n_0	in-situ porosity (-)
n_l	porosity in the sheared zone (-)
Q	average discharge (m^3/s)
R	hydraulic radius (m)
S	energy gradient (-)
T	transport parameter (-)
t_n	specific time of the measurement (s)
U	depth-averaged flow velocity (m/s)
U_{cr}	critical depth-averaged flow velocity (m/s)
u_*	shear stress velocity (m/s)
v_e	the erosion velocity (m/s)
w_s	settling velocity (m/s)
x	horizontal coordinate (cm)
$\triangle$	relative density (-)
Δz_b	difference in bed level (m)
Δt	time interval between two measurements (s)
Φ_p	dimensionless pick-up flux (-)
β	slope angle (deg)
δ	dilatancy factor (-)
κ	Von Karman coefficient (-)
ν	kinematic viscosity (m^2/s)
ϕ	angle of internal repose (deg)
ρ	density of water (kg/m^3)
ρ_s	density of sediment (kg/m^3)
τ	total shear stress (Pa)
τ_b	bed shear stress (Pa)
τ_w	wall shear stress (Pa)
$\tau_{b,cr}$	critical bed shear stress (Pa)
θ	Shields parameter (-)
θ_{cr}	critical Shields parameter (-)

1. Introduction

During breaching of dikes or dams very large flow velocities (i.e. larger than 5 m/s) can be reached (Visser, 1998). Other examples of erosion of sediments at high flow velocities (characterized by high ratios of the erosion velocity and permeability $v_e/k > 3$) are natural erosion due to wave action and currents, especially during stormy conditions. Data from earlier erosion experiments of Gailani *et al.* (2001) and Lemmens (2014, see also Lemmens *et al.* 2016) indicate that significant reductions in erosion rates of a sand bed are possible when bentonite is added to the sand. Bentonite is a very fine grained natural type of clay. The reduction of the erosion rates is effected by the decrease of the permeability of the sand, induced by the swelling of the bentonite particles filling the voids between the sand particles (see Fig. 1). At high flow velocities some of the bentonite will wash out and erode with the sand particles. Since bentonite has a non-toxic, inert nature, this will not harm the aquatic environment.

Lemmens *et al.* (2016) investigated the applicability of a mixture of sand and bentonite in the core of a dike to slow down the process of breaching after failure of the dike. The applicability of a mixture of sand and bentonite as capping material for contaminated bottom sediments, which can be a potential source of significant contamination to the overlying water during storms, was investigated by Gailani *et al.* (2001). Other potential applications could for example be related to scour protection (onshore and offshore) or similar problems. The use of sand-bentonite mixtures could potentially be investigated as counter scour measure in future works. Thus far, the erosion behaviour of sand with bentonite has mainly been tested in small-scale laboratory flumes for flow conditions in the order of 1 m/s (relatively low bed shear stresses). In order to investigate the applicability of a bentonite additive in reducing the erosion velocity at relatively low (1.0 m/s) and relatively high flow velocities (2.0 m/s), the present erosion experiments were carried out. Thirteen different tests were executed, all under supercritical flow conditions. These results provide new insights on the sand's behaviour (with bentonite) for hydrodynamic conditions that are commonly found in storms, by addressing the lack of physical model results on high velocities.

A description is given of the experimental setup, the execution of the tests, the determination of the erosion velocities and the (corrected) bed shear stresses. This is followed by an overview and analysis of the results. Finally, a comparison between the data of the measurements and the erosion model of Van Rhee (2010) is presented.

This article heavily relies on the data and conclusive results found in Foortse (2016), which will not be further referenced in the main text.

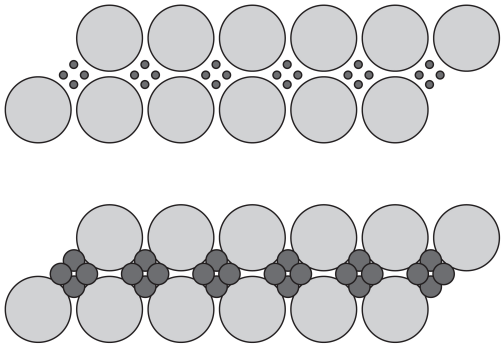

Figure 1. Bentonite is assumed to fill up the the voids and reduce the permeability.

2. Erosion Process

The erosion of sand is characterized by two different regimes: the grain-by-grain (single particle) regime and the dilatancy-reduced erosion regime (see Van Rhee, 2010; Bisschop *et al.*, 2016). The grain-by-grain regime is relevant at relatively low flow velocities, corresponding with relatively low bed shear stresses (often expressed in Shields parameters $<$ 0.5 (see Bisschop *et al.*, 2016) and low ratios of the erosion velocity and permeability (v_e/k <3). The dilatancy-reduced erosion regime starts to dominate at relatively high flow velocities, corresponding with higher bed shear stresses and higher ratios of the erosion velocity and permeability ($v_e/k > 3$). It is not possible to give exact values for the low flow velocities and high flow velocities boundaries, since the ratio of v_e/k determines which regime prevails.

2.1. Grain-by-Grain Erosion

At relatively low flow velocities, erosion models for sand are mainly based on the principle of erosion of single grains (grain by grain erosion). Grain movement starts when the instantaneous fluid force on a grain exceeds the instantaneous resisting force. Shields (1936) has introduced the concept of initiation of motion of individual particles. The condition of initiation of motion is defined as the moment or threshold at which the particles are just starting to move. The balance of lift, drag and gravity forces is given by the Shields parameter θ and is defined as:

$$\theta = \frac{\tau_b}{(\rho_s - \rho) \cdot g \cdot D_{50}} = \frac{u_*^2}{\triangle \cdot g \cdot D_{50}} \tag{1}$$

where $\triangle$ represents the relative density $(\rho_s - \rho)/\rho$, D_{50} is the median diameter of the sediment, u_* is the shear velocity, τ_b the bed shear stress, g is the acceleration of gravity, ρ_s is the density of the grain and ρ is the density of the water. An example of a well-known empirical function for the pick-up flux of sand in the grain-by-grain regime is that of Van Rijn (1984):

$$E = 0.00033 \cdot \rho_s \cdot [\triangle \cdot g \cdot D_{50}]^{0.5} \cdot {D_\star}^{0.3} \cdot T^{1.5} \tag{2}$$

$$D_* = D_{50} \cdot \left(\frac{\triangle \cdot g}{\nu^2} \right)^{1/3} \tag{3}$$

$$T = \frac{\tau_b - \tau_{cr}}{\tau_{cr}} = \frac{\theta - \theta_{cr}}{\theta_{cr}} \tag{4}$$

in which E is the pick-up flux, D_* is the dimensionless particle diameter, ν is the kinematic viscosity of water, T is the transport parameter, τ_{cr} is the critical bed shear stress according to Shields and θ_{cr} is the critical Shields parameter. The pick-up flux E = 0 when $\tau_b < \tau_{cr}$.

2.2. Dilatancy-Reduced Erosion

At relatively high flow velocities, corresponding with higher bed shear stresses and higher ratios of the erosion velocity and permeability ($v_e/k > 3$), the erosion of sand also depends on the properties of the soil mass and not only on the properties of the sand particles. Van Rhee (2010) has explained that this is induced by the behaviour of the sand bed in the erosion process, i.e. that the pickup flux is influenced by the shearing of layers of sand at

the top of the sand bed. The dilative behaviour, resulting from the shearing of the top layers of the sand bed, causes a drop in pore pressure in the top of the sand bed inducing an inflow of water into the sand bed (Fig. 2), which hinders entrainment of sand (dilatancy-reduced erosion). So the permeability has a significant influence on the erosion process. The lower the permeability, the higher the inward hydraulic gradient, the more difficult particles entrain in the water column. Van Rhee (2010) has developed an adapted erosion function for relatively high flow velocities that incorporates these effects via bulk properties like permeability and porosity of the sand bed in an adapted Shields parameter:

$$\theta_{cr}{}^{1} = \theta_{cr}\left(1 + \frac{v_e}{k_l}\frac{n_l - n_0}{1 - n_0}\frac{A}{\triangle}\right) \tag{5}$$

in which v_e is the erosion velocity, k_l is the permeability given a loose soil packing, n_0 is the in-situ porosity, n_l is the porosity in the sheared zone (loose packing) and A is equal to 3/4 for a single particle and approximately 1.7 for a continuum (see Van Rhee, 2010; Van Rhee and Bezuijen, 1992). The modified critical Shields parameter can be used in any conventional erosion function to deal with high velocity regimes as long as the conventional erosion functions contain a critical Shields parameter Van Rhee (2010) and given that the sand-bentonite mixtures behave as a non-cohesive sand (see also Section 3.5).

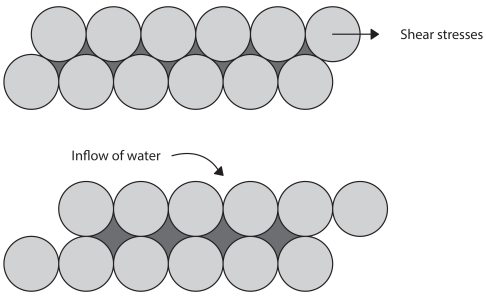

Figure 2. Increase of volume due to shearing; original figure from Van Rhee (2010).

3. Experiments

An experimental program of thirteen different tests was executed in an adapted tilting flume of the Laboratory for Fluid Mechanics of the Delft University of Technology.

3.1. Experimental Set-up

The erosion experiments were carried out in a tilting flume with a length of about 14 m, an effective height of 0.40 m, a width of 0.40 m, and with transparent glass walls on both sides. The maximum inclination of the flume is 1% and the maximum discharge is about 0.025 m^3/s.

The flume was divided into four segments: a wide inflow section including a honeycomb structure to reduce the turbulence and to straighten the flow, an inflow section partly with a fixed concrete bottom, a test section with a sand bed and an outflow section. The width of the flume was reduced to 0.145 m with a smooth plywood wall over almost the entire length of the flume. As a result the flow velocities increased significantly (to a maximum of about 2 m/s). Since the flume is relative narrow compared to the flow depth side-wall corrections were applied to get the effective bed shear stresses (see Section 4.2).

All erosion experiments were performed under supercritical conditions. As a consequence of this flow regime, the preferred equilibrium flow velocities (1 and 2 m/s) were hard to regulate. The equilibrium velocity only depended on the roughness of the sand bed and the slope of the sand bed. The only parameter that could be optimized was the slope of the bed. This resulted in two different setups. One with a slope of 1% and one with an intended equilibrium slope of 3%. The experimental setups are shown in Fig. 3 and in Fig. 4. The first setup, with a bed slope of 1%, had a bed with a height of 0.15 m over the total length of the bed, since the flume was tilted to its maximum inclination of 1%. The second setup, with a bed slope of 3%, had the same 1% inclination from the flume as the previous setup. However, by gradually decreasing the bed level (2 cm/m) in downstream direction a total bed slope of 3% was accomplished.

The height of the bed was chosen to be 0.15 m and the length of the bed was chosen to be about 6 m to give the flow enough length to reach equilibrium conditions so that the slope of the water level would be equal to the slope of the bed.

3.2. Instrumentation

During the experiments the sediment characteristics and the energy gradient were varied. The measurement section was equipped with the following instruments:

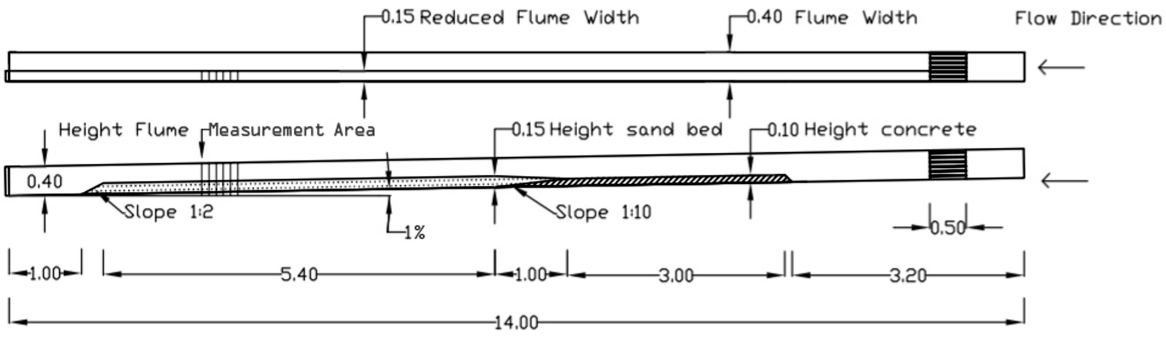

Figure 3. Experimental setup 1 of the erosion test: top view (above) and side view (bottom) with measures in meters.

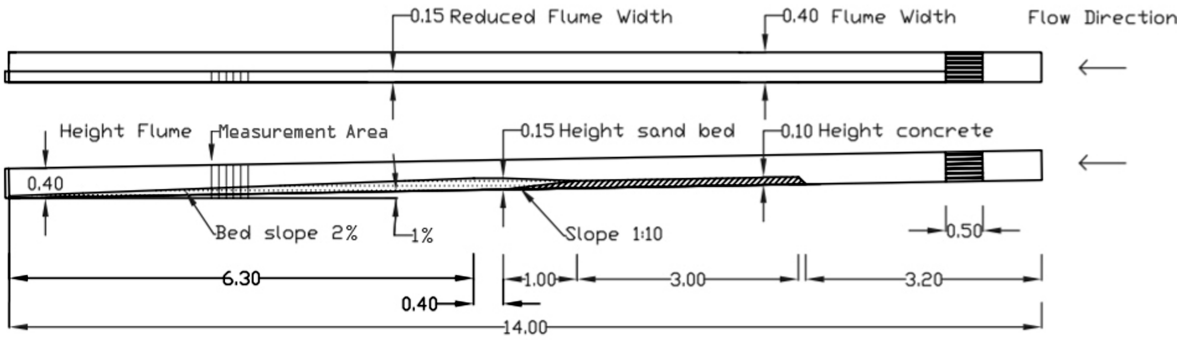

Figure 4. Experimental setup 2 of the erosion test: top view (above) and side view (bottom) with measures in meters.

1. An Electromagnetic Flow meter (EMS) to measure the flow rate as discharged by the pump through the measurement section.
2. Two video cameras to record the water levels and bed levels in the area of interest. To simplify the data analysis a grid was drawn on one of the glass side windows of the flume (Fig. 5). In vertical direction a total height of 0.40 m was divided in parts of 0.01 m and in horizontal direction an area of 0.90 m was divided into parts of 0.10 m. A second camera was positioned on the next window (more upstream) and functioned as a back-up. Clean water tests (to determine the vertical and horizontal velocity profiles) indicated a minimal influence of secondary flow along the walls and indicated uniform flow conditions. Side-wall corrections are applied to compute effective bed shear stresses (see also Section 4.2).
3. An Electromagnetic Flow meter (EMS) to measure the fluid velocity in x-direction, which is the stream direction, at a specific position in the water column. The flow velocity measurements were mainly performed to determine the velocity profile in the flume. During the erosion experiments itself this was not possible, since the equipment created a lot of turbulence.

3.3. Preparation of the Sand-Bentonite Beds

The first step in the preparation of the different beds was to mix bentonite and sand in a dry state as a homogeneous mixture using a concrete mixer. The used type of benonite was Cebogel Sealfix Bentonite (2015). It was added, given a pre-determined mixture ratio, to 50 kg of sand. Since each test roughly needed 200 kg of sand, several batches had to be prepared for each test. Mixtures were prepared with dry volume bentonite contents of 0, 2, 4 and 6 percent. After compaction the sand bed would ideally have an estimated dry bulk density of 1588 kg/m^3 and a corresponding estimated porosity of 0.40. The final step of the preparation phase

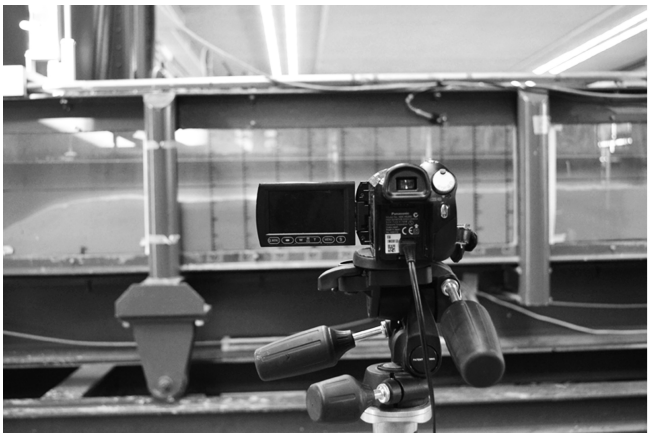

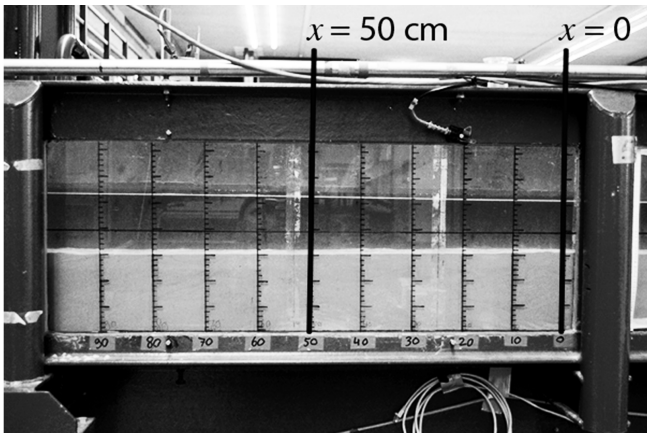

Figure 5. (a) Setup of the camera and (b) Grid on the glass wall in the area of interest.

was to allow the sand bed (including the bentonite) to become saturated with water for a period of about 24 hours. This was specifically needed to activate the bentonite and to let it reach its full swelling capacity.

3.4. Material Properties

Two types of pure quartz sand (M32 sand: D_{50} = 0.256 mm, and S90 sand: D_{50} = 0.150 mm) were used in the experiments. The properties of both sand types are summarized in Table 1. The coefficient of uniformity C_u, defined as: D_{60}/D_{10}, in which D_{10} and D_{60} are the particle diameters at which 10% and 60%, respectively, of the weight of the grains is smaller, were 1.55 and 1.61, respectively. The coefficient of curvature C_c defined as: ${D_{30}}^2/(D_{10}D_{60})$ were 1.07 and 0.94, respectively. This means that both sand types can be characterized as poorly graded.

3.5. Classification of the Mixtures

Classification of fine grained soils is often based on its consistency limits. The consistency of a soil is its physical state at a given moisture content. Four samples of the bed were taken after the erosion tests. According to plastic limit tests (performed according the British Standards (BSI, 1990) the samples were non-plastic, since the plastic limit could not be determined. This means that the sand-bentonite mixtures exhibited no cohesive behavior. In addition, drained direct shear tests were executed to determine the friction angle and (apparent) cohesion of the sand and sand-bentonite mixtures in the Laboratory of Geoscience and Engineering of the Delft University of Technology. The tests were carried out for different dry volume percentages of bentonite (0, 2, 4, 6, 8 and 10%). From the results given in Table 2 it can be concluded that the apparent cohesion for each mixture is small (<3.1 kPa). The friction angle is independent of the volume percentages of added bentonite. It remains in the range of 33.8 to 37.2 degrees for sand with a D_{50} of 0.256 mm and 38.4 to 42.9 degrees for sand with a D_{50} of 0.150 mm. The internal friction angles of the S90 sand type (D_{50} = 0.150 mm) are higher than those of the M32 sand type (D_{50} = 0.256 mm). This is a result of a higher degree of compaction (higher relative density. From these tests it can be concluded that a mixture with a dry volume content of bentonite up to 10% does not show any sign of cohesion-like behaviour and thus still behaves as a non-cohesive sand.

3.6. The Effect of Bentonite on the Permeability

Falling head tests were executed in the Laboratory of Geoscience and Engineering of the Delft University of Technology to determine the permeability of the mixtures with varying bentonite content. Table 3 and Fig. 6 show the results. Adding bentonite clearly reduces the permeability significantly. A 2% dry volume bentonite content already reduces the permeability of the mixture to a value of 20% (or lower) of the original permeabilty for both sand types. Increasing the bentonite content to 6% reduces the permeability to a value of 1% of the original permeability. The reduction in permeability is almost identical for the two different sand types (D_{50} of 0.256 mm and a D_{50} of 150 mm) and suggests that the reduction ratio is almost irrespective of the sand diameter.

4. Experimental Results

	D_{10} (mm)	D_{30} (mm)	D_{50} (mm)	D_{60} (mm)	D_{90} (mm)	C_c (-)	C_u (-)	Characterization
Coarser M32	0.176	0.226	0.256	0.272	0.370	1.07	1.55	poorly graded
Finer S50	0.103	0.127	0.150	0.166	0.236	0.94	1.61	poorly graded

Table 1. Properties of the Sands; from Foortse (2016).

Bentonite Content (%)	Mean Particle Diameter (D_{50}) (mm)	Apparent Cohesion (kPa)	Friction Angle (°)	Initial Porosity (n_0) (-)
0	0.256	1.07	37.1	0.40
2	0.256	0.88	35.6	0.40
4	0.256	1.35	36.5	0.41
6	0.256	1.81	35.3	0.40
8	0.256	2.27	33.8	0.41
10	0.256	2.07	37.2	0.41
0	0.150	3.06	42.9	0.41
2	0.150	2.88	40.0	0.41
4	0.150	2.63	39.3	0.40
6	0.150	3.01	38.4	0.41
8	0.150	2.09	39.4	0.41
10	0.150	2.14	40.2	0.42

Table 2. Results Direct Shear Tests; from Foortse (2016).

Bentonite Content (%)	Mean Particle Diameter (D_{50}) (mm)	Permeability (k) (m/s)	Ratio Permeability / Original Permeability (k/k_0) (-)	Initial Porosity (n_0) (-)
0	0.256	4.8E-4	1.00	0.40
2	0.256	7.3E-5	0.15	0.40
4	0.256	3.2E-5	0.067	0.41
6	0.256	4.7E-6	0.010	0.40
8	0.256	2.3E-6	0.005	0.41
10	0.256	6.1E-7	0.001	0.41
0	0.150	9.9E-5	1.00	0.41
2	0.150	2.1E-5	0.21	0.41
4	0.150	6.3E-6	0.064	0.40
6	0.150	8.1E-7	0.008	0.41
8	0.150	3.5E-7	0.004	0.41
10	0.150	2.5E-7	0.002	0.42

Table 3. Results Permeability Tests; from Foortse (2016).

4.1. Erosion Tests

Thirteen different tests runs were executed. The operational conditions of the thirteen tests are depicted in Table 4. During these tests, the dry volume percentage of bentonite additive, the particle diameter of the sand and the depth-averaged flow velocity were varied. The depth-averaged flow velocity during the erosion tests varied between 1.06 and 2.17 m/s.

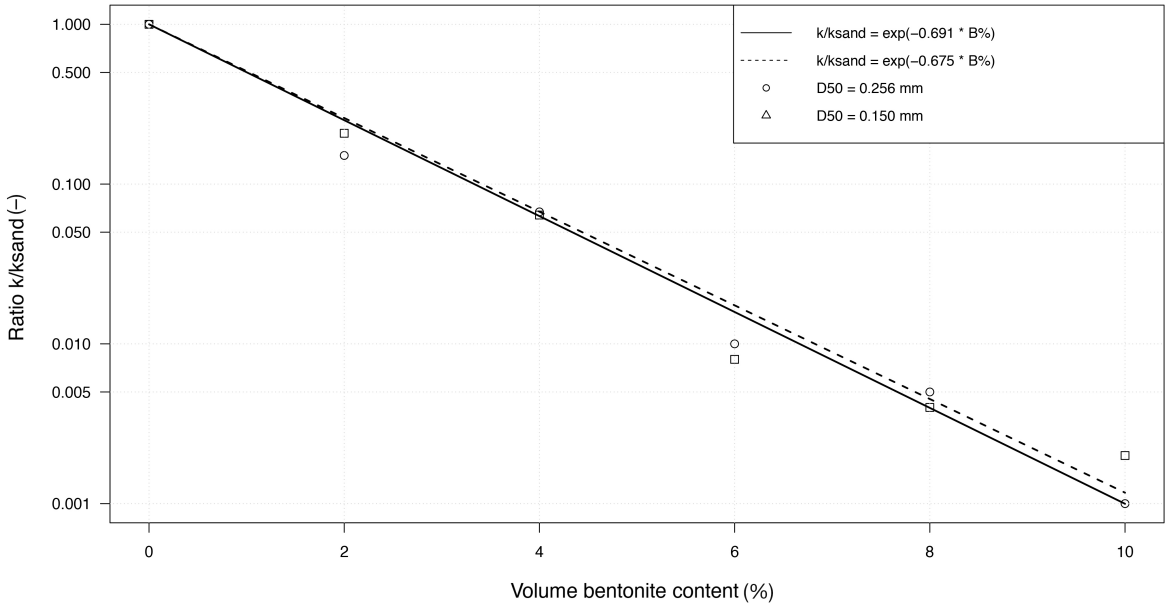

Figure 6. Effect of bentonite on the permeability.

Test	Bentonite Content (%)	Mean Particle Diameter (D_{50}) (mm)	Depth-averaged Flow Velocity (U) (m/s)	Initial Porosity (n_0) (-)
1	0	0.256	1.12	0.40
2	2	0.256	1.06	0.41
3	4	0.256	1.19	0.41
4	6	0.256	1.22	0.41
5	6	0.150	1.10	0.41
6	0	0.150	1.46	0.41
7	0	0.256	2.17	0.40
8	0	0.150	2.01	0.40
9	2	0.256	2.00	0.41
10	4	0.256	2.15	0.41
11	6	0.256	1.72	0.41
12	3	0.150	1.98	0.41
13	0	0.256	1.95	0.41

Table 4. Operational Conditions of the Erosion Tests.

The discharge was constantly measured during the tests and the bed levels and water levels in the area of interest were recorded on video. From the videos the water levels and bed levels were extracted with a Matlab script. The depth-averaged flow velocity U (in x-direction) and the erosion velocity v_e between consecutive frames in time were calculated with Eq. (6) and Eq. (7):

$$U = \frac{Q}{b \cdot h} \quad (6)$$

(7) $$v_e = \frac{z_{b(n)} - z_{b(n+1)}}{t_{n+1} - t_n} = \frac{\Delta z_b}{\Delta t}$$

in which b is the constricted width of the flume, h is the flow depth, Q is the average discharge through the flume, z is the average flow depth in time interval t_{n+1} - t_n, $z_{b(n)}$ is the bed level at a specific time, t_n is the specific time of the measurement, Δz_b is the difference in bed level, and Δt is the time interval between two measurements. For each test run, data from 5 measurement locations (see the measurement area in Fig. 3 and Fig. 4) were analyzed. The measurement locations were all in the area of interest and evenly spaced at a 10 cm interval from each other. The most upstream measurement location was at the x = 0 line of the grid (see Fig. 5).

4.2. Bed Shear Stress

The effective bed shear stress can theoretically be derived from the drop in energy gradient, which is a result of friction losses in the measurement section during the erosion tests. For the correct derivation of the effective bed shear stress, the following effects should be taken into consideration:

1. acceleration of the flow caused by possible non-uniformity;
2. the presence of the side walls.

The erosion velocity directly depends on the bed shear stress. In order to predict the erosion rate in laboratory open-channel flows with good precision, it is necessary to remove side-wall and non-uniformity effects (friction losses) for computing effective bed shear stresses (Cheng and Chua, 2005; Guo, 2014).

In this study the non-uniformity correction was neglected for the tests, since reasonable uniform conditions had developed in the area of interest. Four methods were used to correct the total shear stress for the difference in surface roughness between the eroding sand bed and the walls of the measurement section: the Flow-depth method (Cheng and Chua, 2005), the Hydraulic radius method (Cheng and Chua, 2005), the Vanoni and Brooks (1957) method and the Einstein (1942) method.

1. The flow-depth method (Cheng and Chua, 2005) states that the bed shear stress τ_b causes the following energy loss in the water column per unit area above the bed (see also Guo, 2014):

(8) $$\tau_b = \rho g h S$$

in which S is the energy slope gradient. For narrow flumes the total energy loss above the bed affected by the bottom and side walls becomes:

(9) $$b\tau_b + 2h\tau_w = \rho g b h S$$

in which τ_w is the wall shear stress. This results in the following upper bound expression for the corrected bottom shear stress:

(10) $$\tau_b = \rho g h S - \frac{2h}{b}\tau_w \leq \rho g h S$$

In this study τ_w was estimated using the following expresion:

(11) $$\tau_w = c_f \rho U^2$$

The value of the dimensionless friction coefficient c_f was estimated at roughly 0.0024, depending on the hydraulic radius of the test run.

2. The hydraulic radius method (Cheng and Chua, 2005) states that the bed shear stress τ_b causes the following energy loss in the water column per unit area above the bed (see also Guo, 2014):

(12) $$\tau_b = \rho g R S$$

in which the hydraulic radius R is calculated according to:

(13) $$R = \frac{hb}{2h + b}$$

For narrow flumes with a water depth h and the width of the flume b, the total energy loss above the bed as a result of the bottom and side walls becomes:

(14) $$b\tau_b + 2h\tau_w = (b + 2h)\tau$$

in which τ is the total shear stress. If a rough bed and relatively smooth sidewalls are assumed a lower bound of τ_b is obtained by replacing τ_w by τ_b in Eq.(14) (see Cheng and Chua, 2005):

(15) $$\tau_b > \rho g R S$$

3. The Vanoni and Brooks (1957) method is based on the assumption that the total force loss in a section with smooth and rough wall equals the sum of the force loss along the smooth wall and force loss along the rough wall. This method determines the bed shear stress τ_b by using the bulk friction coefficient f_d (see Eq. (17)), which has a sound theoretical basis. With this friction coefficient the bed shear stress can be expressed as:

$$\tau_b = \frac{b}{b+2h}\frac{f_b}{f_d}\rho g h S \tag{16}$$

with

$$f_d = \frac{8gRS}{U^2} \tag{17}$$

$$f_b = f_d + \frac{2h(f_d - f_w)}{b} \tag{18}$$

$$f_w = \left[20\left(\frac{4UR}{f_d\nu}\right)^{0.1} - 39\right]^{-1} \tag{19}$$

in which f_b is the bed related friction coefficient and f_w is the wall friction coefficient. The wall friction coefficient relation, given by Eq. (19), is obtained by curve fitting and depends on ratio of the Reynolds number over the bulk friction coefficient Re/f_d (see also Cheng and Chua, 2005).

4. The Einstein (1942) method originally accounts for the wall resistance component by correcting the Manning roughness coefficient. The average bed shear stress is defined as:

$$\tau_b = \rho g R S\left(\frac{n_b}{n}\right)^{1.5} \tag{20}$$

where n_b and n are the bed-related and total Manning roughness coefficients, respectively. An alternative form is using the Darcy-Weisbach friction coefficient to account for the effects of the wall friction. It is assumed that the wall-related friction can be estimated using a Blasius expression, which after an extensive substitution and manipulation procedure yields the following corrected bed shear stress (see Cheng and Chua, 2005):

$$\tau_b = \rho g h S\left(1 - \frac{0.114}{b}\left(\frac{U^7\nu}{S^4 g^4}\right)^{0.2}\right) \tag{21}$$

It has been concluded that the values of the corrected bed shear stresses obtained with the four different methods show close resemblance. The differences in shear stress derived with three of the four methods are not very large (Fig. 7). Together with the fact that the Vanoni and Brooks (1957) method is the most widely used method according to literature (Cheng and Chua, 2005), the method of Vanoni and Brooks (1957) has been chosen as the most suitable method to correct for side-wall effects.

4.3. Results

Table 5 presents the results of the thirteen erosion tests including the bed shear stresses, corrected for side-wall effects.

5. Analysis

5.1. Influence of Bentonite on the Erosion Velocity

In order to determine the effectiveness of a bentonite additive on erosion, the erosion velocity of the bed of a sand-bentonite mixture is compared with the erosion velocity of the original sand at the same depth-averaged flow velocity. The effectiveness of the different sand bentonite mixtures is defined as the ratio of the mixture's erosion velocity and the erosion velocity of the original sand:

$$f = \frac{v_{e,mixture}}{v_{e,sand}} \tag{22}$$

The effectiveness is calculated based on the average erosion velocity of each test. Fig. 8 relates the erosion velocity v_e to the depth-averaged flow velocity squared and shows the results for different mixture ratios and sand-types. Linear regression lines through the measurements have also been included, relating the erosion velocity and the depth-averaged flow velocity squared, by assuming that the erosion velocity is proportional to the depth-averaged flow velocity squared $v_e = aU^2$, in which a is the coefficient of the specific regression line. Table 6 contains the linear regression coefficients a of the pure sand and the sand-bentonite mixtures. The effectiveness ratio f for each mixture is then calculated by dividing the mixture's linear regression coefficient and the pure sand linear regression coefficient:

$$f = \frac{a_{mixture}}{a_{sand}} \tag{23}$$

The effectiveness is determined for the coarse sand (D_{50} = 0.256 mm) and the fine sand (D_{50} = 0.150 mm). It is important to note that the regression lines are forced through the origin by specifying

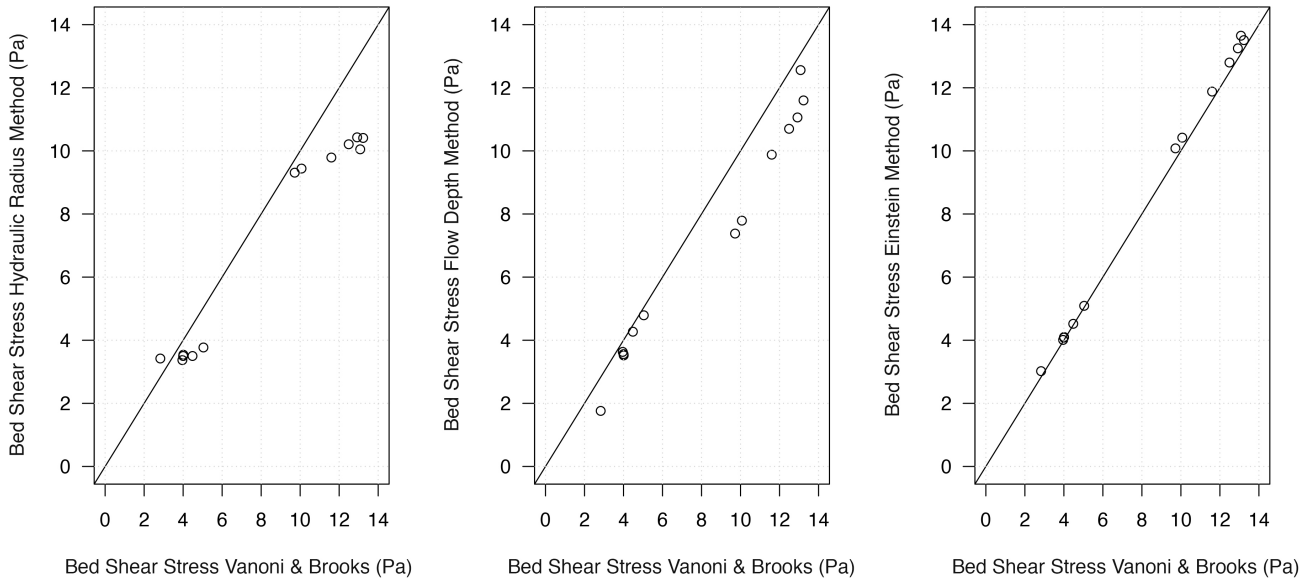

Figure 7. Comparison of the corrected bed shear stresses calculated with the method of Vanoni and Brooks (1957) and the corrected bed shear stresses calculated with the: (left) Hydraulic Radius method, (middle) Flow Depth method, and (right) Einstein (1942) method.

Test	Bentonite Content (%)	Mean Particle Diameter (D_{50}) (mm)	Depth-averaged Flow Velocity (U) (m/s)	Flow Depth (h) (m)	Initial Porosity (n_0) (-)	Erosion Velocity (v_e) (m/s)	Bed Shear Stress (τ_b) (Pa)	Friction Coefficient (f_b) (-)	Roughness Height (k_s) (mm)	Erosion Velocity/ Permeability (v_e/k) (-)
1	0	0.256	1.12	0.065	0.40	4.2E-04	4.0	0.025	0.32	0.87
2	2	0.256	1.06	0.070	0.41	2.8E-04	4.5	0.032	0.75	3.83
3	4	0.256	1.19	0.070	0.41	5.2E-05	4.0	0.023	0.23	1.59
4	6	0.256	1.22	0.072	0.41	2.0E-05	4.0	0.022	0.20	4.29
5	6	0.150	1.10	0.082	0.41	2.8E-05	5.0	0.033	0.93	34.2
6	0	0.150	1.46	0.067	0.41	4.2E-04	2.8	0.011	0.007	4.25
7	0	0.256	2.17	0.056	0.40	7.8E-04	9.7	0.017	0.058	1.62
8	0	0.150	2.01	0.069	0.40	1.1E-03	12.9	0.026	0.36	10.7
9	2	0.256	2.00	0.067	0.41	4.5E-04	12.5	0.025	0.33	6.14
10	4	0.256	2.15	0.058	0.41	3.3E-04	10.1	0.017	0.074	10.0
11	6	0.256	1.72	0.065	0.41	8.5E-06	13.1	0.035	1.01	1.83
12	3	0.150	1.98	0.061	0.41	4.3E-04	11.6	0.024	0.26	-
13	0	0.256	1.95	0.069	0.41	7.2E-04	13.2	0.028	0.49	1.48

Table 5. Erosion Test Results Including (Corrected) Bed Shear Stresses and roughness heights calculated with Eq. (25).

an additional data point (0,0). This is of course a simplification. In reality the erosion velocity v_e is zero if the critical velocity that initiates motion of the sand particles U_{cr} is not yet exceeded. However, since the critical velocity that initiates motion is very low and erosion behaviour at flow velocities $>$ 1 m/s is of main concern in this study, this critical velocity is simplified to be zero (which leads to slightly higher erosion velocities at lower flow velocities). This simplification leads to generic quadratic equations for the erosion velocity in the form of $v_e = aU^2$ and are not verified at flow velocities below 1 m/s. Table 6 and Fig. 8 indicate that significant reductions in erosion velocity are obtained by adding bentonite to a sand mixture. A 2% sand-bentonite mixture already reduces the original erosion velocity by about 50%, a 3% or 4% mixture by 50 to 65% and a 6% mixture at least by 90%. The only

Bentonite Content (%)	Mean Particle Diameter (D_{50}) (mm)	Regression Coefficient (a) (-)	Effectiveness Ratio f (-)
0	0.256	2E-04	1.0
2	0.256	1E-04	0.5
4	0.256	7E-05	0.35
6	0.256	5E-06	0.03
0	0.150	2E-04	1.0
3	0.150	1E-04	0.5
6	0.150	2E-05	0.1

Table 6. Reduction Coefficient f for Several Mixture and Sand Types Based on Linear Regression.

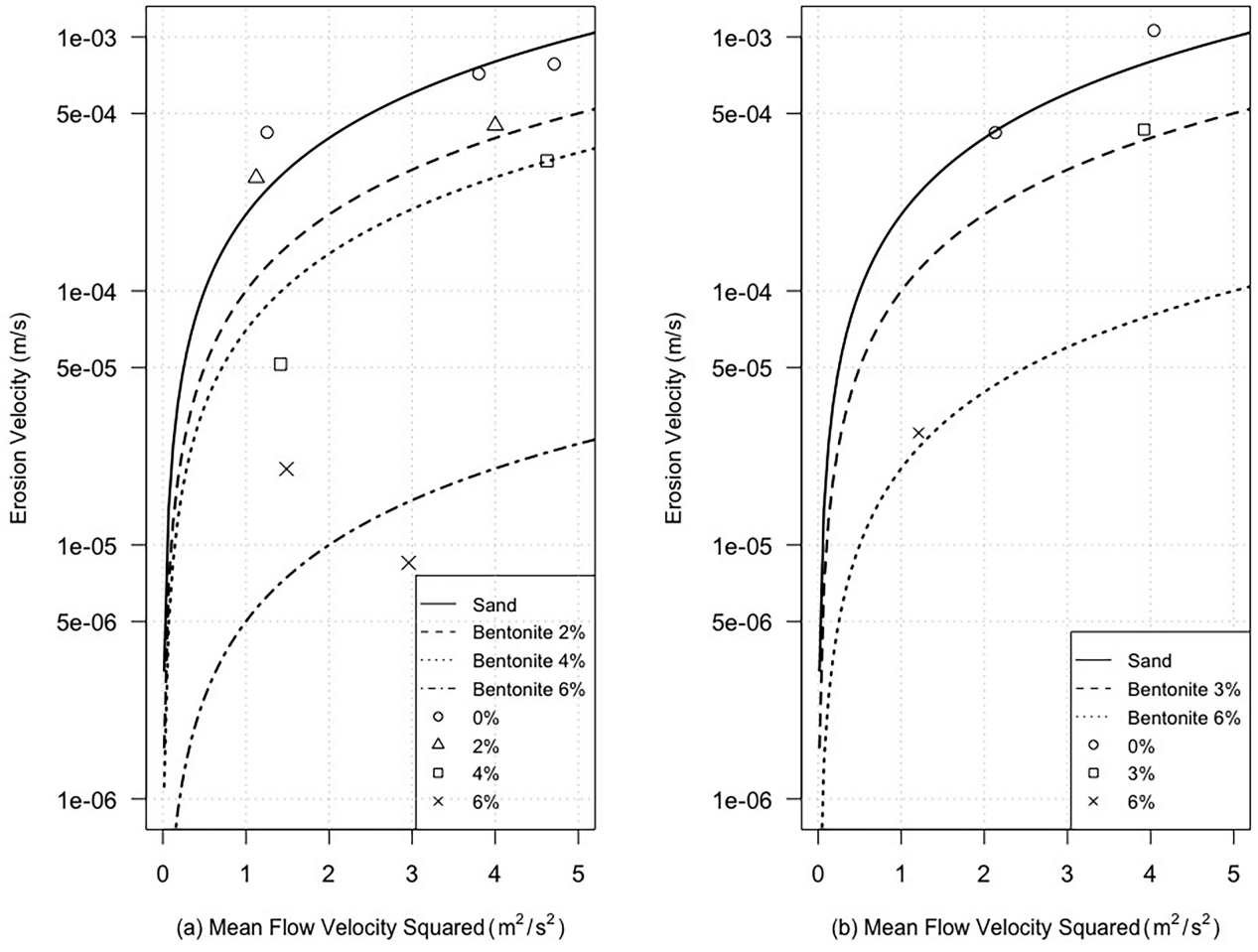

Figure 8. Erosion Velocity as Function of the Depth-Averaged Flow Velocity Squared: (a) D_{50}= 0.256 mm, (b) D_{50}= 0.150 mm.

peculiar result is that of a 6% mixture at a intended depth-averaged flow velocity of about 2 m/s and a D_{50} of 0.256 mm. A possible explanation may be that this is the result of a more homogeneous mixture during this particular test. The more homogeneous the mixture, the better the swelling potential of the bentonite blocking the pores is utilized spatially. This causes a more optimal reduction in permeability and corresponding decrease in erosion velocity.

5.2. Erosion Regime

During the tests the bed shear stress varied between 2.83 Pa and 13.23 Pa (see Table 5), corresponding to a Shields parameter (θ) ranging roughly from 1 to 5. Hence, the flow conditions during the erosion tests can be characterized as dominated by sheet flow conditions ($\theta > 0.5$), indicating that the erosion process was influenced by the properties of the soil mass instead of just the behaviour of single grains. The ratio v_e/k indicates whether dilatancy-reduced erosion is dominant. A value $v_e/k > 3$ is often defined as the starting point of dilatancy-reduced erosion (Van Rhee, 2010). The values for the erosion tests are ranging from 0.87 to 34.2 (see Table 5), indicating that the condition for dilatancy-reduced erosion was not always met. Table 5 shows that the pure sand tests have generally low values (< 3) of v_e/k while the values of v_e/k are generally above 3 for the tests with the sand-bentonite mixtures. Hence, as expected the dilatancy-reduced erosion regime is generally reached faster with sand-bentonite mixtures than with pure sand only.

5.3. Comparison with Existing Data Sets

A literature review regarding the erosion behaviour of sand-bentonite mixtures, has resulted in the conclusion that very few data are available for comparison, i.e. to the best knowledge of the authors only the data of Gailani *et al.* (2001) and Lemmens (2014, see also Lemmens *et al.* 2016) are known. For this reason, the results of experiments executed by Gailani *et al.* (2001) and Lemmens (2014) have been compiled in Table 7 and Table 8. Table 7 shows the results of the erosion experiments of Lemmens (2014) on sand with a D_{50} of 0.208 mm, where the bed shear stress was derived with the Vanoni and Brooks (1957) method. The maximum depth-averaged flow velocity during these experiments was 1.11 m/s. Table 8 shows the results of the erosion experiments of Gailani *et al.* (2001) on sand with a D_{50} of 0.214 mm. An implicit function relating the shear stress and the flow rate for the Sedflume setup (a duct 2 cm in height) was derived in McNeil *et al.* (1996). In the experiments of Gailani *et al.* (2001) the depth-averaged flow velocities reached about 1.58 m/s, with the exception of a test run with a depth-averaged flow velocity of about 2.4 m/s with a bentonite content of 4%. Table 5 shows the results of the present experiments on sand with a D_{50} of 0.256 mm and a D_{50} of 0.150 mm. The bed shear stresses given in Table 5 were also calculated with the Vanoni and Brooks (1957) method. The two datasets are compared with the present experiments based on erosion velocity, bed shear stress, bed related friction coefficient and roughness. The bed related friction coefficient and the bed shear stress are related as follows:

$$\tau_b = \frac{f_b}{8} \cdot \rho \cdot U^2 \tag{24}$$

in which f_b is the bed related friction coefficient. The roughness height k_s and the friction coefficient are related as follows:

$$f_b = \frac{8 \cdot \kappa^2}{\left[ln\left(\frac{12R}{k_s}\right)\right]^2} \tag{25}$$

in which κ is the Von Karman coefficient (=0.40).

The friction coefficients range from 0.011 to 0.035 in the present experiments, resulting in roughness heights ranging from 0.007 to 1.01 mm. The data of the experiments of Lemmens (2014) show friction coefficients ranging from 0.018 to 0.13, resulting in roughness heights ranging from 0.098 to 21.2 mm. The data of Gailani *et al.* (2001) show friction coefficients ranging from 0.018 to 0.063, where it seems that the higher the depth-averaged flow velocity, the lower the friction coefficient. This corresponds with roughness heights ranging from 0.083 to 4.33 mm. The results of Lemmens (2014) have significant fluctuations in friction coefficients and roughness heights, where the 2% bentonite mixtures are resulting in significantly higher roughness heights. More importantly, the friction coefficients and corresponding roughness heights in the data set of Lemmens (2014) are generally an order of magnitude higher than in both the data of the experiments of Gailani *et al.* (2001) and the present experiments. It is worth mentioning that there does not appear to be a clear relationship between the amount of added bentonite and the roughness. In addition, the roughness heights and friction

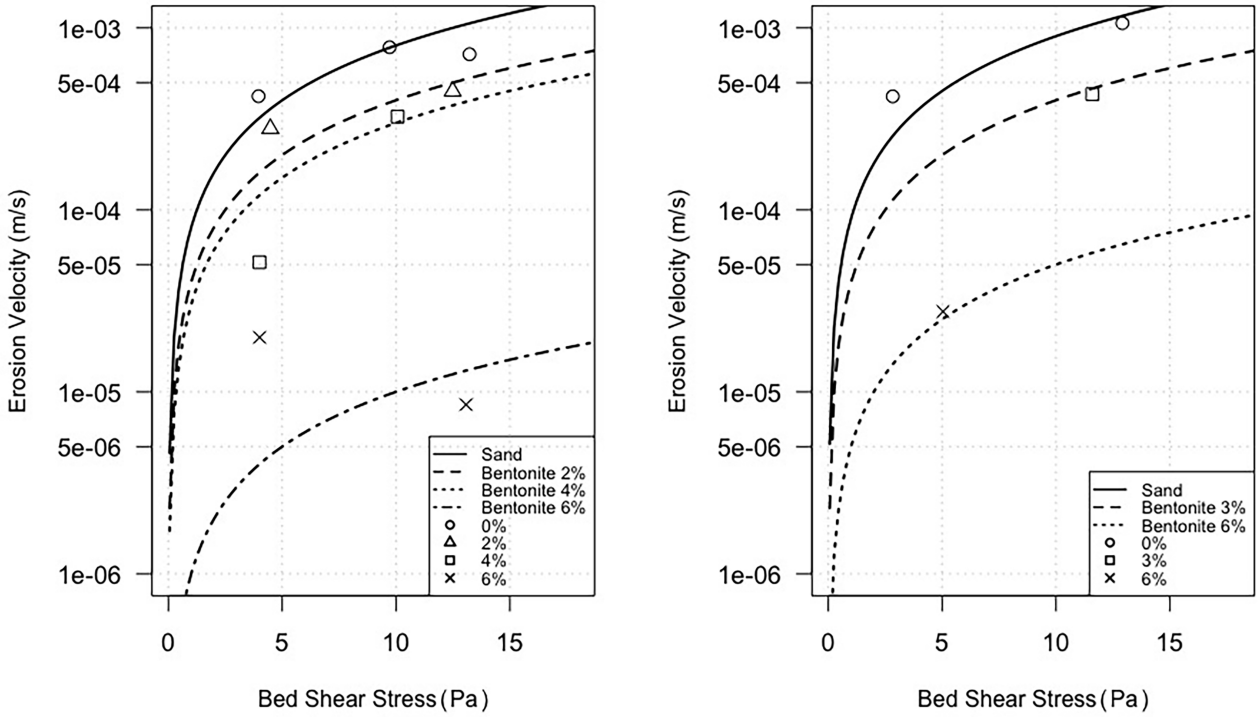

Figure 9. Erosion Velocity as Function of the Bed Shear Stress: (left) D_{50}= 0.256 mm, (right) D_{50}= 0.150 mm.

Bentonite Content (%)	Mean Particle Diameter (D_{50}) (mm)	Depth-averaged Flow Velocity (U) (m/s)	Bed Shear Stress (τ_b) (Pa)	Erosion Velocity (v_e) (m/s)	Friction coefficient (f_b) (-)	Roughness Height (k_s) (mm)
0	0.208	0.82	4.2	8.5E-05	0.049	2.7
2	0.208	0.77	6.7	5.7E-05	0.090	10.1
4	0.208	0.86	1.7	1.4E-05	0.018	0.098
0	0.208	1.06	12.4	2.8E-04	0.088	10.9
2	0.208	0.99	15.8	1.6E-04	0.13	21.2
4	0.208	1.11	7.5	4.4E-05	0.049	2.9

Table 7. Bed Shear Stresses and Friction Coefficients Based on Experimental Data from Lemmens (2014).

coefficients of Gailani *et al.* (2001) and the present experiments generally decrease with increasing flow velocities.

It can also be concluded that the experiments executed by Gailani *et al.* (2001) generally result in higher erosion velocities at similar bed shear stresses than both the data of Lemmens (2014) and the present experiments (see Fig. 9 and Fig. 10). The erosion velocities measured in the present experiments at similar bed shear stresses are generally higher than measured by Lemmens (2014). These differences may be caused by:

1. whether or not applying a side-wall correction;
2. whether or not applying a non-uniformity correction;
3. method used for the side-wall correction;

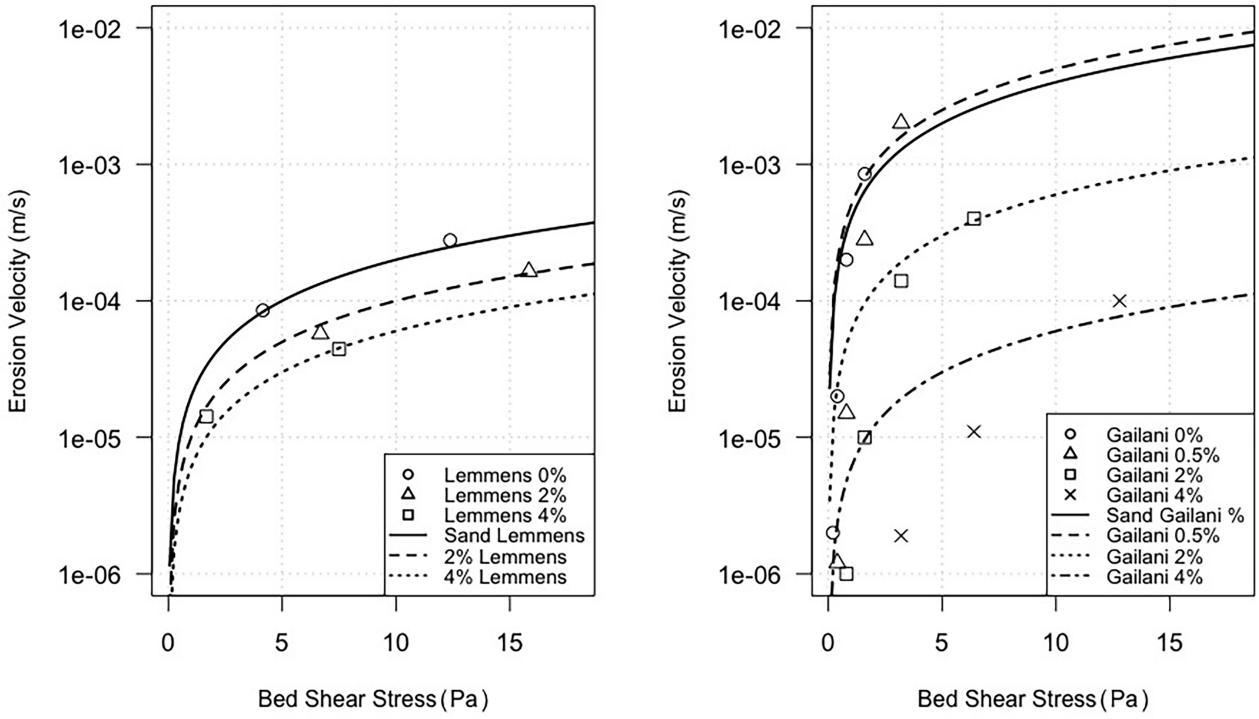

Figure 10. Erosion Velocity as Function of the Bed Shear Stress: (left) D_{50}= 0.208 mm from Lemmens (2014), (right) D_{50}= 0.214 mm from Gailani *et al.* (2001).

4. difference in experimental setup.

For the correct derivation of the effective bed shear stress both the acceleration of the flow caused by possible non-uniformity and the difference in surface roughness between the eroding bed and the wall of the measurement section should be taken into consideration. The significant differences in bed shear stresses are most likely caused by the difficulty in accurately measuring the energy loss of the system. Many methods are available to determine the friction coefficient, which accounts for this energy loss. Some even account for the additional viscosity of the flowing sand-water mixture, because of the high sediment concentrations near the bed. These high sediment concentrations near the bed (and thus higher viscosity) lead to higher energy loss, which is accounted for in the friction coefficient. This means that the particle protrusion is no longer governing and that the roughness is increasing significantly. It is not exactly known how Gailani *et al.* (2001) derived the effective bed shear stresses, which may be an explanation for the difference in results. Lemmens (2014) also used the Vanoni and Brooks (1957) method to determine the bed shear stresses. However, Lemmens (2014) did not apply a non-uniformity correction, whereas no reasonably non-uniform conditions in his tests were apparent. This may be the most important explanation for the difference in results. Lastly, the side-wall correction also influences the corrected bed shear stresses. This correction is related to the depth-averaged flow velocity and has a high impact on the bed shear stress at high velocities. It is hypothesized that the used side-wall correction methods may be over-correcting the bed shear stresses at higher flow velocities and might not be perfectly valid at flow velocities of about 2 m/s and higher.

Bentonite Content (%)	Mean Particle Diameter (D_{50}) (mm)	Depth-averaged Flow Velocity (U) (m/s)	Bed Shear Stress (τ_b) (Pa)	Erosion Velocity (v_e) (m/s)	Friction Coefficient (f_b) (-)	Roughness Height (k_s) (mm)
0	0.214	0.16	0.2	2.0E-06	0.063	4.33
0	0.214	0.32	0.4	2.0E-05	0.031	0.66
0	0.214	0.47	0.8	2.0E-04	0.029	0.52
0	0.214	0.70	1.6	8.5E-04	0.026	0.36
0.5	0.214	0.32	0.4	1.2E-06	0.031	0.66
0.5	0.214	0.47	0.8	1.5E-05	0.029	0.52
0.5	0.214	0.70	1.6	2.8E-04	0.026	0.36
0.5	0.214	1.07	3.2	2.0E-03	0.022	0.21
2	0.214	0.47	0.8	1.0E-06	0.029	0.52
2	0.214	0.70	1.6	1.0E-05	0.026	0.36
2	0.214	1.07	3.2	1.4E-04	0.022	0.21
2	0.214	1.58	6.4	4.0E-04	0.021	0.15
4	0.214	1.07	3.2	1.9E-06	0.022	0.21
4	0.214	1.58	6.4	1.1E-05	0.021	0.15
4	0.214	2.40	12.8	1.0E-04	0.018	0.083

Table 8. Bed Shear Stresses and Friction Coefficients Based on Experimental Data from Gailani *et al.* (2001).

5.4. Comparison with Existing Erosion Function

The test results (see Table 5) are compared with the erosion function of Van Rhee (2010). This erosion function is valid for the grain-by-grain and dilatancy-reduced erosion regime. The erosion function of Van Rhee (2010) reads:

$$v_e = \frac{1}{1 - n_0 - c_b}\left(\Phi_p \sqrt{g \Delta D_{50}} - c_b w_s\right) \tag{26}$$

in which w_s is the settling velocity and c_b the near bed concentration. The dimensionless pick-up flux Φ_p, which is based on the erosion formula of Van Rijn (1984), and the dilatancy factor δ are defined as:

$$\Phi_p = 0.00033 {D_*}^{0.3} \left[\frac{\theta - {\theta_c}^1}{\theta_c^1}\right]^{1.5} \tag{27}$$

$$\delta = \frac{n_1 - n_0}{1 - n_1} \frac{1}{\triangle(1 - n_0)} \tag{28}$$

where θ_c^1 is defined as:

$${\theta_c}^1 = \theta_c \left[\frac{sin(\phi - \beta)}{sin(\phi)} + \delta \frac{v_e}{k_l}\right] \tag{29}$$

in which, ϕ is the angle of internal repose and β is the slope angle. Eq. (29) is similar to Eq. (5) for the continuum approach, but now also includes the effect of a sloping surface.

The erosion function of Van Rhee (2010) is compared with the experimental erosion velocities in Fig. 11. Here, the near-bed concentration c_b is estimated to range from 0.03 to 0.20 depending on the magnitude of the bed shear stress and the sediment diameter. The angle of internal friction ϕ is 36 ° (coarse sand) or 40 ° (fine sand), the slope angle β is 0, the porosity n_0 is 0.40, the porosity in the sheared zone (loose packing) n_l is chosen to be 0.48 and the values of the permeability k are obtained from Table 3. In order to get a reasonable fit for the coarse sand the permeability had to be divided by 3 (an empirical reduction coefficient). This empirical reduction coefficient may be accounting for uncertainties in:

1. the type of sand;
2. the value of the near bed concentration;
3. the difference between the in-situ and loose state permeability.

Fig. 11 shows that the agreement between the erosion function of Van Rhee (2010) and the experimental data is reasonable, after some corrections of the magnitudes of the permeability of the sand-bentonite beds. The general trend is reflecting the influence of bentonite on the erosion velocity, especially for bentonite contents up to 4%. Generally, the erosion function is correctly predicting the erosion velocities of the finer sand and over-predicting the erosion

velocities of the coarser sand (without correction). However, less experimental observations for the finer sand type are available.

6. Conclusion

At high flow velocities (>1 m/s) dilatancy may hinder erosion and a relatively low permeability will restrict the erosion rate. An experimental program including thirteen different erosion tests was executed to study the reduction of the erosion of sand at relatively high flow velocities (>1 m/s) with a bentonite additive. In order to determine the effectiveness of a bentonite additive in reducing the erodibility of sand, the erosion velocity of a sand-bentonite mixture was compared with the erosion velocity of pure sand at the same depth-averaged flow velocity. The results show that significant reductions in erosion velocity are obtained by adding bentonite to a sand mixture. A 2% sand-bentonite mixture reduces the original erosion velocity by about 50%, a 3% or 4% mixture by 50 to 65% and a 6% mixture at least by 90%. This reduction in erosion velocity is a direct consequence of the decrease in permeability, which is caused by the swelling potential of the bentonite blocking the pores. The comparison of an existing erosion function, valid for high-velocity erosion, with the present experimental data shows the trend of the erosion velocity as function of the permeability k and the depth-averaged flow velocity U. However, corrections of the magnitudes of the permeability of the sand-bentonite beds containing the coarser sand (D_{50} = 0.256 mm) were necessary. The erosion function and the experimental data show good agreement when the sand-bentonite beds contain the finer sand (D_{50} = 0.150 mm) and thus no corrections of the magnitudes of the permeability of the sand-bentonite beds containing the finer sand were necessary.

The difference in results of the present experiments, the data of Gailani *et al.* (2001) and the data of Lemmens (2014) is most likely caused by the difficulty in accurately measuring the energy loss of the system. Lemmens (2014) did not apply a non-uniformity correction, whereas no reasonably non-uniform conditions in his tests were apparent and Gailani *et al.* (2001) performed their tests in a duct 2 cm in height.

Acknowledgements

We thank the reviewers for their careful review and relevant suggestions to improve the manuscript.

REFERENCES

Bisschop F, Miedema SA, Visser PJ, Keetels GH, van Rhee C and Verhagen HJ (2016) Experiments on the pickup flux of sand at high flow velocities. *Journal of Hydraulic Engineering,* 142(7), 572-582. doi: 10.1061/(ASCE)HY.1943-7900.0001142. .

BSI (1990) Methods of test for soils for civil engineering purposes. classification tests. In *BS 1377-2:1990*, BSI.

Cebo Holland BV (2015) Cebo Sealfix. Cebo Holland BV, IJmuiden, The Netherlands, http://www.cebo.com/nederland/nl/bentoniet/cebogel-sealfix.html.

Cheng NS and Chua LHC (2005) Comparison of sidewall correction of bed shear stress in open-channel flows. *Journal of Hydraulic Engineering* **131(7)**: 605–609. doi: 10.1061/(ASCE)0733–9429(2005)131:7(605).

Einstein HA (1942) Formulas for the transportation of bed load. *Transactions of ASCE,* 107(1), 561-577 .

Foortse B (2016) *Retardation of breach growth under high flow velocities*. M.S. thesis, Delft University of Technology, Delft, The Netherlands. (https://repository.tudelft.nl/islandora/search/?collection=education).

Gailani JZ, Jin L, McNeil J and Lick W (2001) Effects of bentonite on sediment erosion rates. *DOER Technical Notes Collection* (ERDC TN-DOER-N9), U.S. Army Engineer Research and Development Center, Vicksburg, MS, USA .

Guo J (2014) Sidewall and non-uniformity corrections for flume experiments. *Journal of Hydraulic Research,* 53(2), 218-229. doi: 10.1080/00221686.2014.971449 .

Lemmens DDMM (2014) *Design of a breach retardant dike*. M.S. thesis, Delft University of Technology, Delft, The Netherlands. (https://repository.tudelft.nl/islandora/search/?collection=education).

Lemmens DDMM, Bisschop F, Visser PJ and van Rhee C (2016) Retarding the breaching process of dikes. *Proceedings of the Institution of Civil Engineers - Maritime Engineering,* 169(3), 99-114. doi:10.1680/jmaen.2015.20 .

McNeil J, Taylor C and Lick W (1996) Measurements of erosion of undisturbed bottom sediments with depth. *Journal of Hydraulic Engineering* **122(6)**: 316–324.

Shields A (1936) Anwendung der Ähnlichtkeitsmechanik und der Turbulenzforschung auf die Geschiebebewegung. *Mitteilungen der Preussische Versuchsanstalt für Wasserbau und Schiffbau* **26**: 524–526, Heft 26, Berlin, Germany.

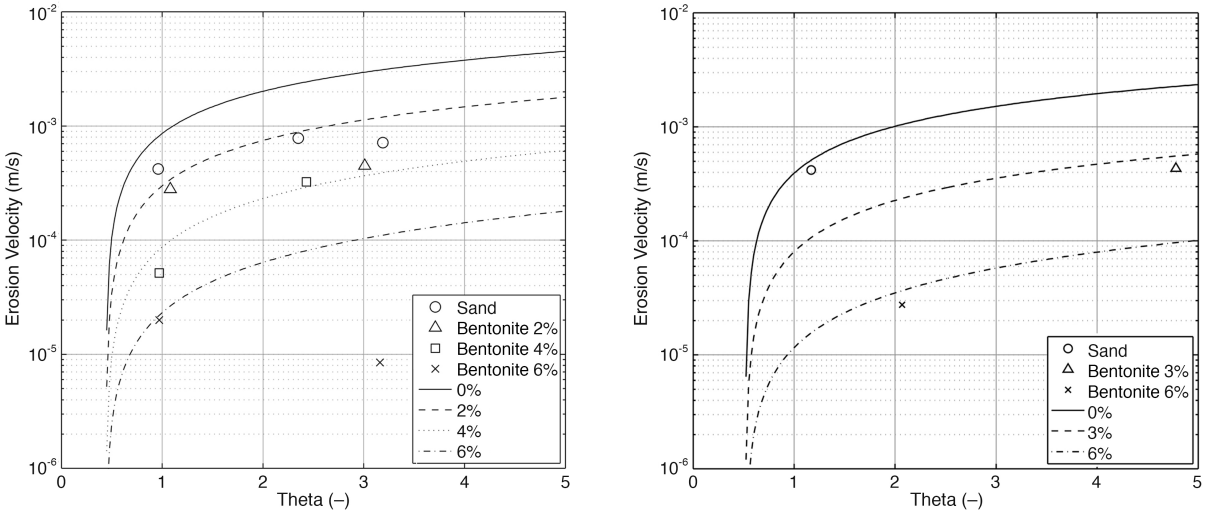

Figure 11. Comparison of the erosion function of Van Rhee (2010) with the experimental data: (left) D_{50}= 0.256 mm, (right) D_{50}= 0.150 mm.

Van Rhee C (2010) Sediment entrainment at high flow velocity. *Journal of Hydraulic Engineering,* 136(9), 572-582. doi: 10.1061/(ASCE)HY.1943-7900.0000214 .

Van Rhee C and Bezuijen A (1992) Influence of seepage on the stability of a sandy slope. *J. Geotech. Engrg.,* 118(8), 1236–1240 .

Van Rijn LC (1984) Sediment pick-up functions. *Journal of Hydraulic Engineering* **110(10)**: 1494–1502.

Vanoni VA and Brooks NH (1957) Laboratory studies of the roughness and suspended load of alluvial streams. Technical report, Sedimentation Laboratory, California Institute of Technology, Pasadena, California, U.S.A. .

Visser PJ (1998) *Breach growth in sand-dikes*. PhD thesis, Delft University of Technology, The Netherlands.